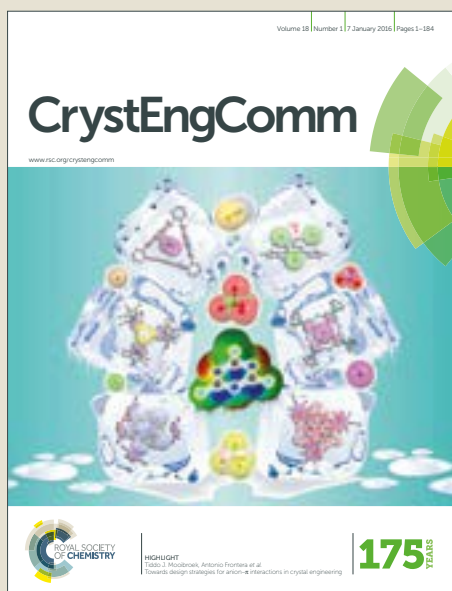


CrystEngComm

Accepted Manuscript



This article can be cited before page numbers have been issued, to do this please use: M. Liu, H. Yu and Z. Liu, *CrystEngComm*, 2019, DOI: 10.1039/C9CE00034H.



This is an Accepted Manuscript, which has been through the Royal Society of Chemistry peer review process and has been accepted for publication.

Accepted Manuscripts are published online shortly after acceptance, before technical editing, formatting and proof reading. Using this free service, authors can make their results available to the community, in citable form, before we publish the edited article. We will replace this Accepted Manuscript with the edited and formatted Advance Article as soon as it is available.

You can find more information about Accepted Manuscripts in the [author guidelines](#).

Please note that technical editing may introduce minor changes to the text and/or graphics, which may alter content. The journal's standard [Terms & Conditions](#) and the ethical guidelines, outlined in our [author and reviewer resource centre](#), still apply. In no event shall the Royal Society of Chemistry be held responsible for any errors or omissions in this Accepted Manuscript or any consequences arising from the use of any information it contains.

A Pair of Homochiral Trinuclear Zn (II) Clusters Exhibiting Unusual Ferroelectric Behaviour at High-Temperature

Meiying Liu, Haiyang Yu and Zhiliang Liu*

Received 00th January 20xx,
Accepted 00th January 20xx

DOI: 10.1039/x0xx00000x

www.rsc.org/

Molecular ferroelectrics as a class of promising information storage materials have triggered widespread attention owing to their light weight, easy processing and mechanical flexibility. However, reports of molecular ferroelectrics with high-temperature ferroelectric behaviour and the higher spontaneous polarization are mainly focus on organic–inorganic perovskites, and which is scarce in coordination compound avenues. Here, a pair of homochiral trinuclear Zn (II) clusters formulated as R-[Zn₃(R-L)₂(CH₃COO)₄] (**R-1**) and S-[Zn₃(S-L)₂(CH₃COO)₄] (**S-1**), were successfully constructed with zinc (II) and the enantiomeric chiral Schiff-base ligands (R/S)-HL (HL = 2-methoxy-6-[(1-phenyl-ethylimino)-methyl]-phenol) through solvent diffusion method. The solid-state circular dichroism (CD) spectra perfectly illustrate the enantiomeric characteristic of **R-1** and **S-1**. Interestingly, the trinuclear Zn (II) cluster (**R-1**) exhibits unusual high-temperature ferroelectric behaviour at 503 K, when external electric field is 12 KV/cm, remnant polarity (P_r) and spontaneous polarization (P_s) of **R-1** can reach up to 5.4 μC/cm² and 8.45 μC/cm², respectively, which can be comparable with organic–inorganic perovskite ferroelectrics in the literatures. To the best of our knowledge, it is the first example of high-temperature ferroelectric possessing the higher spontaneous polarization in Zn-based molecular ferroelectrics.

Introduction

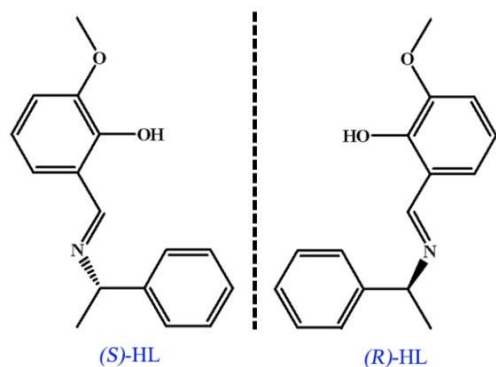
For decades, polynuclear complexes or clusters have already intrigued chemists' attention owing to their underlying applications in sensors, magnetism, optics, chirality and ferroelectric or dielectric materials.^{1–12} In the scope of ferroelectric materials, bifunctional systems integrating ferroelectric properties with optical activity, chirality, magnetism, fluorescence, dielectric or piezoelectric properties have been reported.^{13–20} In order to attain versatile multifunctional ferroelectric materials, it is necessary to rationally design and controllably synthesize the specific complexes or clusters. In light of that chiral space groups and polar point groups are the essential conditions for ferroelectric materials, it may be an optimal choice to utilize homochiral ligand to synthesize ferroelectric polynuclear clusters with the addition of other potential properties such as circular dichroism, fluorescence, magnetism and so on. Among chiral ligands, chiral Schiff-base ligand is an extremely popular candidate due to its unique advantages such as extensive coordination sites, abundant coordination modes and simple synthetic methods.²¹ What's more, polynuclear cluster ferroelectrics as an emerging class of ferroelectrics will be

more competitive than perovskite ferroelectrics, because they can be synthesized through moderate chemistry approach, and exhibit plentiful molecular structures, tuneable chemical and physical properties. For example, Jérôme Long et al reported a high-temperature molecular ferroelectric Zn/Dy cluster exhibiting single-ion-magnet behaviour and lanthanide luminescence.¹⁷ Thomas. C. W. Mak et al researched a chiral 3D Metal–Organic Framework presenting ferroelectric switchable behaviour through fast reversible re/adsorption of water spirals.²² Therefore, it may be a great research area using clusters to explore multifunctional properties such as chirality, ferroelectricity, fluorescence, magnetism and so on. Based on aforementioned considerations, we have successfully synthesized a pair of homochiral trinuclear Zn (II) clusters which were fabricated through a pair of enantiomerically chiral Schiff-base ligands with divalent zinc salt using solvent diffusion method. The chiral Schiff-base ligands (Scheme 1), stemmed from the condensation of 2-hydroxy -3-methoxybenzaldehyde and R/S-2-amino-3-phenyl-1- propanol, will be beneficial to clusters crystallized in the polar point groups compatible with the structural necessity of ferroelectrics. As rarely reported multifunctional ferroelectric materials, first, fluorescent properties of **R-1** and **S-1** have been researched displaying blue-green light emission by solid fluorescence spectra. Then, the solid-state circular dichroism (CD) spectra perfectly explain the enantiomeric characteristic of **R-1** and **S-1**. Finally, the trinuclear Zn (II) clusters belong to polar space group that it is an indispensable requirement for ferroelectric. It's striking that the trinuclear Zn (II) cluster (**R-1**) exhibits well-shaped hysteresis loop at high-temperature of

Inner Mongolia Key Laboratory of Chemistry and Physics of Rare Earth Materials, School of Chemistry and Chemical Engineering, Inner Mongolia University, Hohhot 010021, P.R. China. E-mail: cezliu@imu.edu.cn. Fax/Tel: +86-471-4994375.

*Electronic Supplementary Information (ESI) available: [details of any supplementary information available should be included here]. See DOI: 10.1039/x0xx00000x

503K, which is extremely unusual high-temperature ferroelectric behaviour in coordination compound perspective. Simultaneously, the spontaneous polarization (P_s) reaches to $8.45 \mu\text{C}/\text{cm}^2$ at high-temperature of 503 K, which can be competitive with organic-inorganic perovskite-type ferroelectrics reported in the literatures.^{23, 24} As far as we know, this is the first example of high-temperature ferroelectric possessing the higher spontaneous polarization in Zn-based molecular ferroelectrics.



Scheme 1 The enantiomeric Schiff-base ligands (R/S)-HL

Experiment

Materials and Measurements

All chemicals were purchased from commercial sources and used without further purification. Elemental analyses of C, H and N were tested on a Perkin-Elmer 2400 elemental analyzer. Infrared spectra were collected by the FT-IR spectrometer using KBr pellets under the range of $4000\text{--}400 \text{ cm}^{-1}$. Power X-ray diffraction (PXRD) patterns were measured on an EMPYREAN PANALYTICAL apparatus with single crystals power in the range of $5\text{--}80^\circ$ using $\text{Cu-K}\alpha$ radiation. Circular dichroism spectra were conducted on a JASCO J-810 Spectropolarimeter in KBr tables in the wavelength range of $200\text{--}650 \text{ nm}$. TG curves were attained with a NETZSCH STA409pc apparatus under a heating rate of $10^\circ\text{C}/\text{min}$ from 20 to 1300°C in the nitrogen protection. Fluorescence spectra for **R-1** and **S-1** were recorded on an Hitachi F-7000 FL Spectrophotometer equipped with a 150 W xenon lamp as the excitation and emission source at room temperature, and the slit width of ligand's fluorescence spectra both are 5.0 nm in the excitation and emission, and that of Zn-clusters are 5.0 nm in the excitation and 2.5 nm in the emission. Fluorescence decay lifetimes were carried out by Edinburgh FLS920 spectrophotometer. The $P\text{--}E$ hysteresis loop and leakage current curves were performed at high temperature using a Premier II ferroelectric instrument and 9010 Temperature Controller. Temperature dependence of the dielectric constant was measured through E4980A Precision impedance analyzer. The high temperature electric polarization, dielectric constant and leakage current curves were measured using pellet, which was pressed using crystal power, coated with silver paste on two opposite surfaces.

Synthesis of Schiff-base ligand (R/S)-HL

The Schiff-base ligand was synthesized by the following method. R/S(\pm)-1-Phenylethylamine (10 mmol, 0.89 g) was dissolved in methanol solution (5 mL), and then the methanol solution (5 mL) including o-vanillin (10 mmol, 1.52 g) was added under refluxing. After 2 hours, the light-yellow solution containing required product was obtained and used without further purification.

Synthesis of $R\text{-}[\text{Zn}_3(\text{R-L})_2(\text{CH}_3\text{COO})_4]$ (**R-1**)

The Schiff-base ligand (R)-HL (1.0 mmol) was added in ethanol (10 mL) including triethylamine (1.0 mmol, $140 \mu\text{L}$), and then $\text{Zn}(\text{CH}_3\text{COO})_2 \cdot 2\text{H}_2\text{O}$ (0.5 mmol, 0.10 g) was added. The mixture was stirred for 30 min at room temperature, next to the mixture was filtered. The filtrate was transferred to the tube and diffused across the n-hexane. Yellow block crystals were attained after about 4 days, which were collected through filtering and air-drying. Yield: 50% (based on $\text{Zn}(\text{CH}_3\text{COO})_2 \cdot 2\text{H}_2\text{O}$). Elemental analysis calcd for **R-1** ($\text{C}_{40}\text{H}_{44}\text{N}_2\text{O}_{12}\text{Zn}_3$): C, 51.06%, H, 4.71% and N, 2.98%. Found: C, 50.56%, H, 4.22%, and N, 2.89%. IR (KBr pellet, cm^{-1}): 3442s, 2976m, 2378s, 1623s, 1455w, 1407w, 1310w, 1244m, 1215m, 1090m, 977w, 859w, 738w, 702m, 669m.

Synthesis of $S\text{-}[\text{Zn}_3(\text{S-L})_2(\text{CH}_3\text{COO})_4]$ (**S-1**)

S-1 was synthesized in the same condition with **R-1**, except that the Schiff-base ligand (S)-HL (1.0 mmol) was used instead of the Schiff-base ligand (R)-HL (1.0 mmol). Yield: 52% (based on $\text{Zn}(\text{CH}_3\text{COO})_2 \cdot 2\text{H}_2\text{O}$). Elemental analysis calcd for **R-1** ($\text{C}_{40}\text{H}_{44}\text{N}_2\text{O}_{12}\text{Zn}_3$): C, 51.06%, H, 4.71% and N, 2.98%. Found: C, 50.53%, H, 4.18%, N, 2.83%. IR (KBr pellet, cm^{-1}): 3441s, 2978m, 2376s, 1622s, 1456w, 1408w, 1311w, 1245m, 1216m, 1091m, 978w, 859w, 738w, 702m, 670m.

Crystal data collection and refinement

Crystallographic datas of **R-1** and **S-1** were collected on a Bruker Apex II diffractometer equipped with a CCD area detector and graphite-monochromatic $\text{Mo-K}\alpha$ radiation ($\lambda = 0.71073 \text{ \AA}$). Absorption corrections were applied using the SADABS program. Structures were solved by direct methods and refined by the full-matrix least-squares method on F^2 . All non-hydrogen atoms were refined with anisotropic thermal parameters, while all hydrogen atoms were added to appropriate positions in theory and refined with isotropic thermal parameters by a riding model. Crystallographic data have been deposited at the Cambridge Crystallographic Data Center with the deposition numbers CCDC 1813074 for **R-1** and CCDC 1813076 for **S-1**.

Results and discussion

Description of the structures

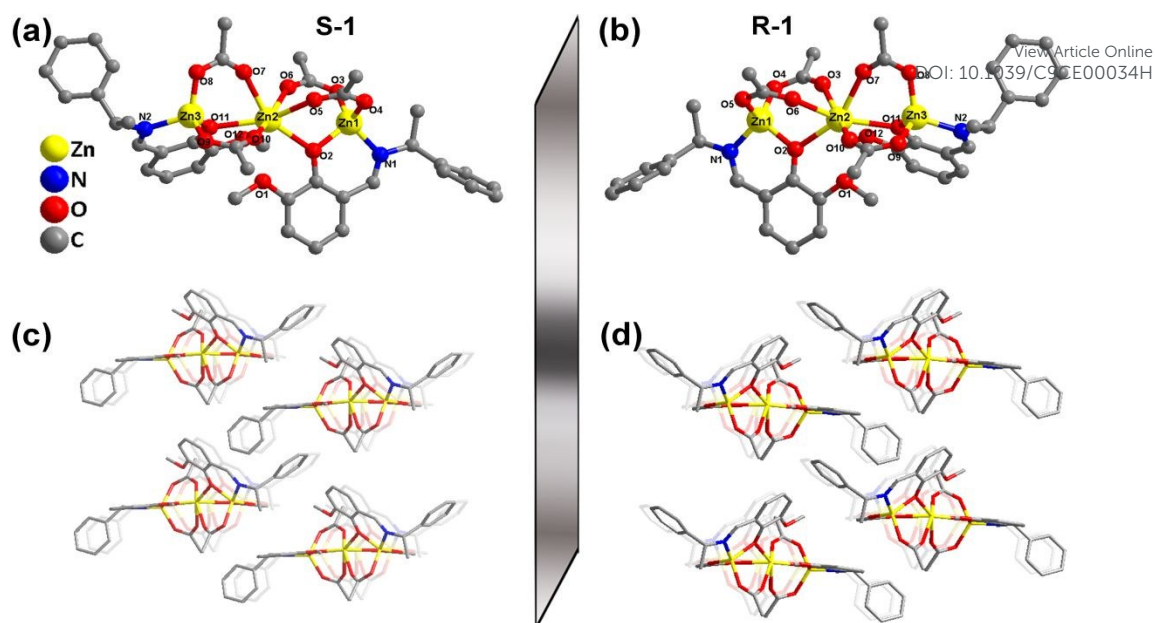


Fig. 1 Molecular structure of trinuclear Zn(II) clusters **S-1** (a) and **R-1** (b), packing view of trinuclear Zn(II) clusters **S-1** (c) and **R-1** (d), displaying four crystallographically independent cluster. Hydrogen atoms are omitted for clarity, Zn (yellow), N (blue), O (red), C (gray)

Single-crystal X-ray diffraction analysis verified that **R-1** and **S-1** are enantiomeric crystallizing in monoclinic space group $P2_1$ belonging to polar point group, which proves the chirality has been effectively transferred from the chiral ligand to clusters. Considering the structures of **R-1** and **S-1** are basically similar, **R-1** was selected as representative to describe the specific crystal structure in detail. As shown in Fig. 1, in the asymmetric unit, there are three independent Zn(II) ions which adopts two different coordination fashions. Both Zn1 and Zn3 are four-coordinated with quadrihedron coordination geometry, ligated by one nitrogen atom and one oxygen atom from one (R)-L⁻ ligand, and two oxygen atoms from two different carboxyl groups. The Zn1–O/N bond distances are in the range of 1.934(3)–2.020(5) Å and the O–Zn1/3–O and O–Zn1/3–N bond angles are 95.05(17)–115.63(18)°, which is comparable to these Zn(II) complexes in other literatures.^{25, 26} Zn2 adopts a distorted octahedral geometry, coordinated by two oxygen atoms from two different (R)-L⁻ ligands, and four oxygen atoms from four different carboxyl groups. The Zn2–O/N bond lengths ranging from 2.357(4)–2.427(4) Å, the O–Zn2–O and O–Zn2–N bond angles are 74.60(13)–159.63(15)°, all of that are comparable to these in other reported Zn(II) compounds.^{27, 28} The adjacent Zn(II) ions are bridged by two μ_2 - η^1 : η^1 carboxylate group and one μ_2 -phenol-oxygen, forming a linear trinuclear structure. The distances between the central Zn(II) ion and two terminal Zn(II) ions are 3.5327(10) Å and 3.5075(11) Å, respectively, and which is similar to the analogous Zn(II) complexes.²⁹ The coordination fashions of **S-1** and **R-1** are basically similar with analogue complex in literatures, which are six-coordinated with octahedron geometry, five-coordinated with square pyramid configuration or four-coordinated with quadrihedron coordination geometry. The packing diagram of analogue Zn(II) complexes almost are 2D or 3D structure,^{25–29} while the packing diagram of trinuclear Zn(II) clusters exhibits the linear stacked arrangement as shown in Fig.1(c) and Fig.1(d). The

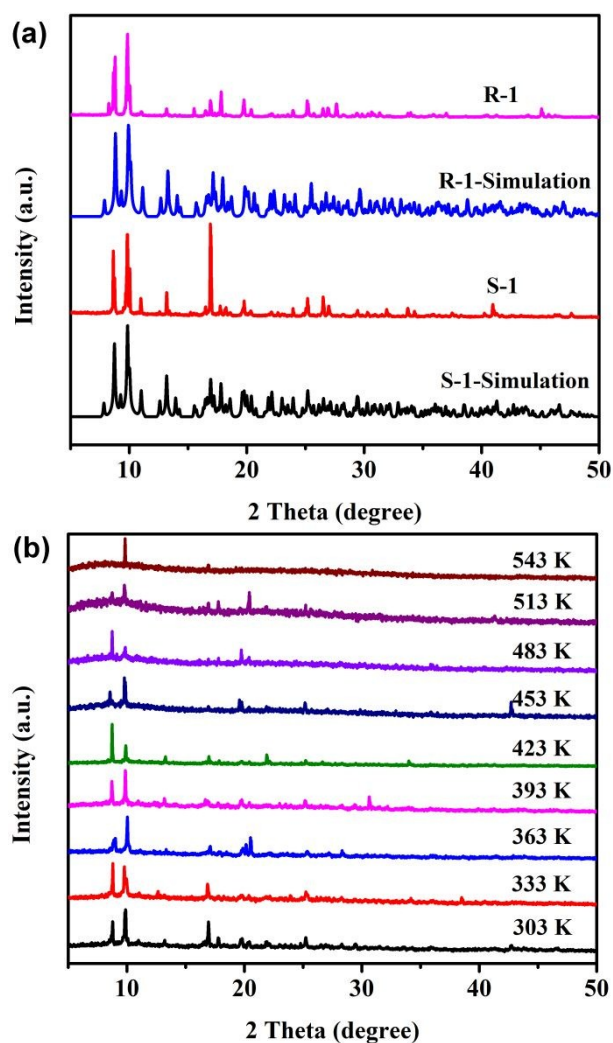


Fig. 2 PXRD patterns for **S-1** and **R-1** (a), PXRD patterns of **R-1** at different temperatures (b)

reason of that may be caused by the difference of ligands. Crystallographic data and structure refinement parameters for **S-1** and **R-1** are listed in Table S1, the main bond lengths (Å) and bond angles (°) for **S-1** and **R-1** are listed in Table S2 and Table S3. In Fig.2(a), all of main patterns of as-synthesized Zn(II) clusters are basically consistent with the simulated patterns, though there exists some small patterns unwell corresponded to the simulation. The phenomenon might be explained by following reasons. (i) There is little impurity in crystal power. (ii) The crystal is weathering in some extent. (iii) Some solvent molecules might volatilize in the surface of crystal. (iv) The simulation of Zn-cluster is obtained by the Single-crystal X-ray diffraction analysis utilizing the single-crystal, while the PXRD of that is measured using the power grinded by single-crystal. The tiny difference of single-crystal and crystal power may cause the distinction between the simulated patterns and PXRD of as-synthesized sample.

CD spectra and Thermal stability study

To prove optical activity and enantiomeric nature, solid-state circular dichroism (CD) spectra of **R-1** and **S-1** were measured. As shown in Fig.3, the spectra of **R-1** and **S-1** are roughly mirror images of each other, which clearly illustrate the characters of a pair of optical enantiomeric. The spectra of **R-1** displays a negative Cotton effect around 333 and 414 nm, while **S-1** presents a positive Cotton effect at the same wavelength. The thermogravimetric analysis (TGA) was tested to inspect the stability of **R-1** (Fig.S3). There is about 2.5% weight loss in the range of 300-528 K. After analysis and calculation, there is no free solvent molecule in the crystal lattice. Therefore, it may be caused by minor impurity adhering to the surface of crystal. When the temperature is above 528 K, the curve start quickly decreasing, illustrating the structure of **R-1** starts disintegrated. Moreover, the **R-1** can remain greatly structural stability until decomposition, which is verified by PXRD at different temperature (Fig.2b). When the temperature increases, the PXRD of **R-1** almost remain unchanged until it was destroyed.

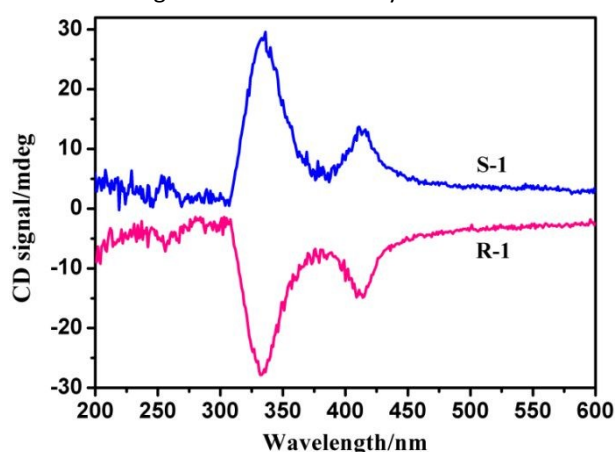


Fig.3 CD spectra for **S-1** and **R-1** at RT in KBr pellets

Ferroelectric and dielectric properties

The structural analysis reveals that both **R-1** and **S-1** are polar space group $P2_1$, which belongs to one of ten polar point groups (C_1 , C_2 , C_{1h} , C_{2v} , C_4 , C_{4v} , C_3 , C_{3v} , C_6 , C_{6v}) required for

presenting ferroelectricity.³⁰ In light of the enantiomeric nature of **R-1** and **S-1**, **R-1** was selected to research ferroelectric and dielectric properties. Dielectric measurement of **R-1** was carried out on pellet pressed by utilizing crystal powder under the temperature range of 300 – 550 K (Fig.4a), the dielectric constant doesn't exhibit obviously abnormal in

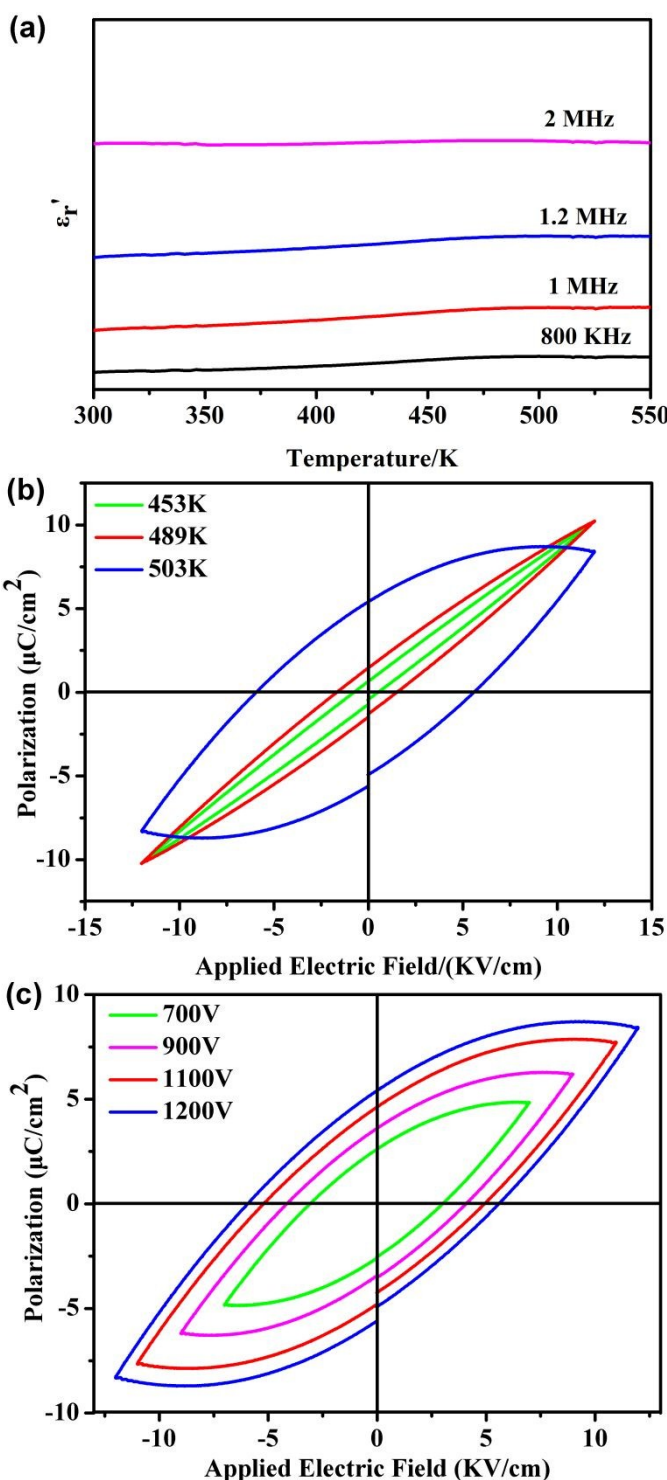


Fig.4 Temperature dependence of the dielectric constant for **R-1** (a), Hysteresis loop (100 Hz) for **R-1** obtained from pellet pressed using crystal powder at different temperatures (b), Hysteresis loop (100 Hz) for **R-1** under different external electric fields at 503 K (c)

the range of temperature, indicating no phase transition appears before **R-1** start decomposing, which is consistent with the PXRD at different temperature and DSC analysis (Fig.S4). The hysteresis loop was performed up to 503 K, while the hysteresis loop of **R-1** wasn't discovered at room temperature, which may illustrate the electric field required to efficiently polarize **R-1** is too high.¹⁷ With temperature rising, polarity of **R-1** gradually increases but still is unsaturated. When it is up to 503 K, **R-1** shows a well-shaped hysteresis loop (Fig.4b). As shown in Fig.4c, both remnant polarity and saturated polarity increasingly goes up with increasing applied electric field. When external electric field is 12 KV/cm, remnant polarity (P_r) and spontaneous polarization (P_s) of **R-1** can reach up to 5.4 $\mu\text{C}/\text{cm}^2$ and 8.45 $\mu\text{C}/\text{cm}^2$, respectively. Such a high polarization is significantly higher than that of the classical ferroelectric Rochelle salt ($P_s = 0.25 \mu\text{C}/\text{cm}^2$)³¹ and some Zn-based molecular ferroelectrics,^{20,32-41} but is in the same order of magnitudes for several perovskite-type molecular ferroelectrics, such as [MeHdabco]RbI₃ ($P_s = 6.8 \mu\text{C}/\text{cm}^2$)²³ or (3-pyrrolinium)CdBr₃ ($P_s = 7.0 \mu\text{C}/\text{cm}^2$).²⁴ Moreover, the low leakage current (less than $10^{-7} \text{ A}/\text{cm}^2$) as a function to further corroborate the P - E hysteresis loops of **R-1** originating from the ferroelectricity (Fig.S5).^{17,42-44} As far as we know, it is the first Zn-based molecular ferroelectric which possesses the higher spontaneous polarization and exhibits high-temperature ferroelectric property (Table 1).

Fluorescence properties of **R-1** and **S-1**

The fluorescence properties of the ligand have been researched (Fig.S6), and the sharp emission peak of (S)-HL and (R)-HL both are at 406 nm ($\lambda_{\text{ex}} = 283 \text{ nm}$). Both **S-1** and **R-1** exhibit greatly strong blue-green fluorescence under UV irradiation in the solid state at room temperature. As shown in Fig.S7, the broad emission peak of **S-1** and **R-1** both are at 460 nm ($\lambda_{\text{ex}} = 327 \text{ nm}$). Generally, fluorescence can derive from metal-centered emission (extensively observed in lanthanide complexes by the so-called antenna effect), organic ligands excitation (especially from the highly conjugated ligands) and charge-transfer such as ligand-to-metal charge transfer (LMCT) and metal-to-ligand charge transfer (MLCT).² Furthermore, it is very difficult to oxidize or reduce Zn^{2+} belonging to the d^{10} configuration, so the fluorescence of **S-1** and **R-1** is not charge-transfer in nature.⁴⁵⁻⁴⁷ Comparing to the emission peak of ligand and trinuclear Zn (II) clusters, the emission peaks of **S-1** and **R-1** exhibit red-shift in some degree. Thus, the fluorescence of **S-1** and **R-1** may be ascribed to the ligands fluorescence emissions. What's more, after coordination between the ligand and Zn (II) ion, the conjugation effect has been enhanced leading the stronger emission intensity of **S-1** and **R-1** than that of (S)-HL and (R)-HL. Moreover, the fluorescent lifetime of **R-1** and **S-1** are 2.35 and 2.41 μs , respectively (Fig.S8). And the quantum yields both are 2.4%.

Table 1. The list of measured temperature, remnant polarity (P_r) and spontaneous polarization (P_s) in some Zn-based ferroelectrics

Compound	Temperature (K)	P_r ($\mu\text{C}/\text{cm}^2$)	P_s ($\mu\text{C}/\text{cm}^2$)	Reference
^a R-[Zn ₃ (R-L) ₂ (CH ₃ COO) ₄]	503 K	5.4	8.45	This work
^b {[Zn ₂ (TIPA)(btc)(μ_2 -OH)]·4H ₂ O} _n	283 K	0.02	0.066	32
^c [Zn ₂ (X)(CH ₃ CH ₂ OH)]·3H ₂ O	283 K	0.01	-	33
^d [Zn ₂ (mtz)(nic) ₂ (OH)] _n ·0.5nH ₂ O	RT	2.9	6.26	34
^e [Zn(phtz)(nic)] _{2n}	RT	2.5	5.27	34
^f [Zn(HQA)Br ₂ (H ₂ O) ₃] _n	RT	0.16	0.30	35
^g R-[Zn ₄ (HL) ₂ (L) ₂ ·(CH ₃ OH) ₂ ·(NO ₃) ₂]	RT	3.97	15.3	36
^h [Zn ₂ (tib) _{4/3} (L ¹) ₂ ·DMA]	RT	0.032	-	37
ⁱ {[Zn ₆ (MIDPPA) ₃ (1,2,4-btc) ₃ (NO ₂) ₃ (H ₂ O) ₃](H ₂ O) ₇] _n	RT	0.058	0.127	20
^j ZnL ₂ (H ₂ O) ₂	RT	0.128	0.25	38
^k [Zn(s-nip) ₂] _n	RT	0.035	0.294	39
^l [Zn ₃ (BIDPE) ₃ (5-OH-bdc) ₃ ·4H ₂ O] _n	RT	0.033	0.105	40
^m [Zn(Mitz)Cl] _n	RT	0.21	0.51	41

^a HL = 2-methoxy-6-[(1-phenyl-ethylimino)-methyl]-phenol, ^b TIPA = tris[4-(1H-imidazol-1-yl)-phenyl]amine, H₃btc = 1,3,5-benzenetricarboxylic acid, ^c H₄X = tetrakis[4-(carboxyphenyl)oxamethyl]methane acid, ^d Hmtz = 5-methyltetrazole, Hnic = nicotinic acid, ^e Hphtz = 5-phenyltetrazole, Hnic = nicotinic acid, ^f HQA = 6-methoxyl-(8S,9R)-cinchonan-9-ol-3-carboxylic acid, ^g H₂L = 2-[(1-benzyl-2-hydroxy-ethylimino)-methyl]-6-methoxy-phenol, ^h H₂L¹ = biphenyl-4,4'-dicarboxylic acid, tib = 1,3,5-tris(1-imidazolyl)benzene, ⁱ MIDPPA = 4,4'-di(4-pyridine)-4''-imidazoletriphenylamine, 1,2,4-H₃btc = 1,2,4-benzenetricarboxylic acid, ^j L = 1,2,2-trimethyl-3-(pyridin-4-ylcarbamoyl)cyclopentanecarboxylic acid, ^k s-nip = (S)-2-(1,8-naphthalimido)-3-(4-imidazole)propanoate, ^l BIDPE = 4,4'-bis(imidazol-1-yl)diphenyl ether, 5-OH-H₂bdc = 5-hydroxy-isophthalic acid, ^m Mitz = 3-tetrazolyl-6-methyl-5-(4-pyridyl)-2-pyridone
RT = room temperature

Conclusions

In summary, a pair of homochiral trinuclear Zn (II) clusters, exhibiting unusual high-temperature ferroelectric behaviour, has been obtained by assembling the chiral Schiff-base ligands with divalent zinc salt using solvent diffusion method. The

trinuclear Zn (II) cluster (**R-1**) presents excellently thermal stability up to 528 K. Meanwhile, the trinuclear Zn (II) clusters (**R-1** and **S-1**) present obvious fluorescence properties, showing blue-green emission. What's more, the chirality of the clusters is demonstrated by solid-state circular dichroism (CD) spectra. It is worth mentioning that the trinuclear Zn (II) cluster (**R-1**) can display well-shaped hysteresis loop at high-

temperature of 503 K, which is extremely scarce high-temperature ferroelectric behaviour. When external electric field is 12 KV/cm, remnant polarity (P_r) and spontaneous polarization (P_s) of **R-1** can reach up to 5.4 $\mu\text{C}/\text{cm}^2$ and 8.45 $\mu\text{C}/\text{cm}^2$, respectively. The spontaneous polarization of **R-1** is much higher than most that of reported Zn-based molecular ferroelectrics and is on a par with some high-temperature perovskite-type ferroelectrics. As far as we know, it is the first example of high-temperature Zn-based molecular ferroelectric possessing an impressive spontaneous polarization. It can be seen from the above mentioned that the pair of homochiral trinuclear Zn (II) clusters facilitate the development of molecular-based multifunctional materials for ferroelectrics, fluorescence property and excellent thermal stability materials.

Conflicts of interest

There are no conflicts to declare.

Acknowledgements

We are grateful for the financial support provided by the NSFC of China (21761023) and the Inner Mongolia Autonomous Region Fund for Natural Science (2017ZD01).

Notes and references

- G. F. Ji, J. J. Liu, X. C. Gao, W. Sun, J. Z. Wang, S. L. Zhao, Z. L. Liu, *J. Mater. Chem. A*, 2017, **21**, 10200-10205.
- Y. Cui, Y. Yue, G. Qian and B. Chen, *Chem. Rev.*, 2012, **112**, 1126-1162.
- M. Guo, X. Yan, Y. Kwon, T. Hayakawa, M.-a. Kakimoto and T. Goodson, *J. Am. Chem. Soc.*, 2006, **128**, 14820-14821.
- C.-L. Hu and J.-G. Mao, *Coord. Chem. Rev.*, 2015, **288**, 1-17.
- L.-L. Han, X.-Y. Zhang, J.-S. Chen, Z.-H. Li, D.-F. Sun, X.-P. Wang and D. Sun, *Cryst. Growth Des.*, 2014, **14**, 2230-2239.
- S. Li, X. S. Du, B. Li, J. Y. Wang, G. P. Li, G. G. Gao and S. Q. Zang, *J. Am. Chem. Soc.*, 2018, **140**, 594-597.
- M. Mon, J. Ferrando-Soria, M. Verdaguier, C. Train, C. Paillard, B. Dkhil, C. Versace, R. Bruno, D. Armentano and E. Pardo, *J. Am. Chem. Soc.*, 2017, **139**, 8098-8101.
- X.-P. Wang, W.-M. Chen, H. Qi, X.-Y. Li, C. Rajnák, Z.-Y. Feng, M. Kurmoo, R. Boča, C.-J. Jia, C.-H. Tung and D. Sun, *Chem. Eur. J.*, 2017, **23**, 7990-7996.
- S. Yuan, Y.-K. Deng, W.-M. Xuan, X.-P. Wang, S.-N. Wang, J.-M. Dou and D. Sun, *CrystEngComm*, 2014, **16**, 3829.
- A. M. Polgar, F. Weigend, A. Zhang, M. J. Stillman and J. F. Corrigan, *J. Am. Chem. Soc.*, 2017, **139**, 14045-14048.
- Y. Shen, C.-C. Fan, Y.-Z. Wei, J. Du, H.-B. Zhu and Y. Zhao, *Cryst. Growth Des.*, 2016, **16**, 5859-5868.
- J. Wu, L. Zhao, L. Zhang, X. L. Li, M. Guo and J. Tang, *Inorg. Chem.*, 2016, **55**, 5514-5519.
- D. W. Fu, W. Zhang and R. G. Xiong, *Dalton Trans.*, 2008, 3946-3948.
- W. Gao, Z. Zhang, P. F. Li, Y. Y. Tang, R. G. Xiong, G. Yuan and S. Ren, *ACS nano*, 2017, **11**, 11739-11745.
- A. K. Gupta, D. De, R. Katoch, A. Garg and P. K. Bharadwaj, *Inorg. Chem.*, 2017, **56**, 4697-4705.
- P. F. Li, Y. Y. Tang, Z. X. Wang, H. Y. Ye, Y. M. You and R. G. Xiong, *Nat. commun.*, 2016, **7**, 13635.
- J. Long, J. Rouquette, J. M. Thibaud, R. A. Ferreira, L. D. Carlos, B. Donnadiu, V. Vieru, L. F. Chibotaru, J. Konczewicz, J. Haines, Y. Guari and J. Larionova, *Angew. Chem. Int. Ed.*, 2015, **54**, 2236-2240.
- Y. Sun, Z. Hu, D. Zhao and K. Zeng, *Nanoscale*, 2017, **9**, 12163-12169.
- J. Yang, L. Zhou, J. Cheng, Z. Hu, C. Kuo, C. W. Pao, L. Jang, J. F. Lee, J. Dai, S. Zhang, S. Feng, P. Kong, Z. Yuan, J. Yuan, Y. Uwatoko, T. Liu, C. Jin and Y. Long, *Inorg. Chem.*, 2015, **54**, 6433-6438.
- M. D. Zhang, Y. L. Li, Z. Z. Shi, H. G. Zheng and J. Ma, *Dalton Trans.*, 2017, **46**, 14779-14784.
- Z.-X. Wang, L.-F. Wu, X.-K. Hou, M. Shao, H.-P. Xiao and M.-X. Li, *Z. Anorg. Allg. Chem.*, 2014, **640**, 229-235.
- X. Y. Dong, B. Li, B. B. Ma, S. J. Li, M. M. Dong, Y. Y. Zhu, S. Q. Zang, Y. Song, H. W. Hou and T. C. Mak, *J. Am. Chem. Soc.*, 2013, **135**, 10214-10217.
- W. Y. Zhang, Y. Y. Tang, P. F. Li, P. P. Shi, W. Q. Liao, D. W. Fu, H. Y. Ye, Y. Zhang and R. G. Xiong, *J. Am. Chem. Soc.*, 2017, **139**, 10897-10902.
- P. F. Li, W. Q. Liao, Y. Y. Tang, H. Y. Ye, Y. Zhang and R. G. Xiong, *J. Am. Chem. Soc.*, 2017, **139**, 8752-8757.
- M. Xue, G. Zhu, Y. Zhang, Q. Fang, I. J. Hewitt and S. Qiu, *Cryst. Growth Des.*, 2008, **8**, 427-434.
- X.-X. Zhou, H.-C. Fang, Y.-Y. Ge, Z.-Y. Zhou, Z.-G. Gu, X. Gong, G. Zhao, Q.-G. Zhan, R.-H. Zeng and Y.-P. Cai, *Cryst. Growth Des.*, 2010, **10**, 4014-4022.
- H. Li, B. Zhao, R. Ding, Y. Jia, H. Hou and Y. Fan, *Cryst. Growth Des.*, 2012, **12**, 4170-4179.
- J.-J. Shen, M.-X. Li, Z.-X. Wang, C.-Y. Duan, S.-R. Zhu and X. He, *Cryst. Growth Des.*, 2014, **14**, 2818-2830.
- L. Chen, W.-K. Dong, H. Zhang, Y. Zhang and Y.-X. Sun, *Cryst. Growth Des.*, 2017, **17**, 3636-3648.
- P. P. Shi, Y. Y. Tang, P. F. Li, W. Q. Liao, Z. X. Wang, Q. Ye and R. G. Xiong, *Chem Soc Rev.*, 2016, **45**, 3811-3827.
- J. Valasek, *Phys. Rev.*, 1921, **17**, 475-481.
- X.-Q. Yao, J.-S. Hu, M.-D. Zhang, L. Qin, Y.-Z. Li, Z.-J. Guo and H.-G. Zheng, *Cryst. Growth Des.*, 2013, **13**, 3381-3388.
- Z. Guo, R. Cao, X. Wang, H. Li, W. Yuan, G. Wang, H. Wu and J. Li, *J. Am. Chem. Soc.*, 2009, **131**, 6894-6895.
- D.-S. Liu, Y. Sui, W.-T. Chen and P. Feng, *Cryst. Growth Des.*, 2015, **15**, 4020-4025.
- H. Zhao, Q. Ye, Z. R. Qu, D. W. Fu, R. G. Xiong, S. D. Huang and P. W. Chan, *Chem.*, 2008, **14**, 1164-1168.
- H. Yu, M. Liu, X. Gao and Z. Liu, *Polyhedron*, 2017, **137**, 217-221.
- Y. Wang, Y. Qi, V. A. Blatov, J. Zheng, Q. Li and C. Zhang, *Dalton Trans.*, 2014, **43**, 15151-15158.
- Q. Huang, J. Yu, J. Gao, X. Rao, X. Yang, Y. Cui, C. Wu, Z. Zhang, S. Xiang, B. Chen and G. Qian, *Cryst. Growth Des.*, 2010, **10**, 5291-5296.
- L. Yu, X.-N. Hua, X.-J. Jiang, L. Qin, X.-Z. Yan, L.-H. Luo and L. Han, *Cryst. Growth Des.*, 2014, **15**, 687-694.
- J. Hu, L. Huang, X. Yao, L. Qin, Y. Li, Z. Guo, H. Zheng and Z. Xue, *Inorg. Chem.*, 2011, **50**, 2404-2414.
- Y. Z. Tang, M. Zhou, J. Huang, Y. H. Tan, J. S. Wu and H. R. Wen, *Inorg. Chem.*, 2013, **52**, 1679-1681.
- Z. Su, J. Fan, T.-a. Okamura, W.-Y. Sun and N. Ueyama, *Cryst. Growth Des.*, 2010, **10**, 3515-3521.
- Y. Sui, D. P. Li, C. H. Li, X. H. Zhou, T. Wu and X. Z. You, *Inorg. Chem.*, 2010, **49**, 1286-1288.
- D.-P. Li, T.-W. Wang, C.-H. Li, D.-S. Liu, Y.-Z. Li and X.-Z. You, *Chem. Commun.*, 2010, **46**, 2929.
- L. Wen, Y. Li, Z. Lu, J. Lin, C. Duan and Q. Meng, *Cryst. Growth Des.*, 2006, **6**, 530-537.
- L. Wen, Z. Lu, J. Lin, Z. Tian, H. Zhu and Q. Meng, *Cryst. Growth Des.*, 2007, **7**, 93-99.

Journal Name

ARTICLE

47 L. P. Zhang, J. F. Ma, J. Yang, Y. Y. Pang and J. C. Ma, *Inorg. Chem.*, 2010, **49**, 1535-1550.

View Article Online
DOI: 10.1039/C9CE00034H

Table of Contents Entry

View Article Online
DOI: 10.1039/C9CE00034H

A pair of homochiral trinuclear Zn (II) clusters exhibit unusual ferroelectric behaviour at high-temperature.

